

STUDIES OF THE EFFECTS OF LASER BEAM MODE CONSIDERED BY NUMERICAL SIMULATION OF WELDING PERFORMANCE FOR MICRO WELDING OF THIN AL SHEET BY Nd:YAG

Şef lucr. dr. ing. Ioan-Sorin LEOVEANU
Universitatea „Transilvania”, Braşov



Este absolvent al Universităţii „Transilvania” din Braşov, Facultatea de Tehnologia Construcţiilor de Maşini, Secţia utilajul şi tehnologia sudării. A efectuat stagiul la U. „Tractorul” din Braşov şi la I.P.T. Întorsura Buzăului, apoi a fost inginer proiectant la Institutul de Cercetare pentru Autovehicule şi Tractoare – Braşov, la departamentul punţi motoare directe. Din 1988 este cadru didactic la Universitatea „Transilvania” din Braşov, la Catedra de ingineria materialelor şi sudării. Este doctor inginer al Universităţii „Politehnica” din Bucureşti, din 2002. A contribuit la proiectarea punţilor motoare cu mare unghi de virare pentru tractoare agricole şi industriale, la proiectarea şi omologarea structurilor de rezistenţă sudate pentru tractoare industrial si agricole. A publicat manuale şi monografii pe plan local, central şi în colaborare cu universităţi din străinătate, precum şi articole în reviste şi buletinele unor conferinţe de specialitate din ţară şi din străinătate.

REZUMAT. Sudarea cu laser Nd:YAG a tablelor subţiri din aliaje de Al impune condiţionări severe privind gradientii termici generaţi de sursa laser în piesele ce formează îmbinarea. În cazul utilizării sursei laser în modul continuu este extrem de greu de asigurat stabilitatea geometriei îmbinării sudate din cauza dificultăţii în menţinerea constant a intensităţii sursei laser şi în poziţionarea acesteia în zona îmbinării. Aceasta este cauza adoptării modului pulsatoriu pentru sursa termică. Rezolvarea problemelor legate de variaţia coeficientului de absorbţie a căldurii generate de sursa termică, între aproximativ 8% pentru cazul atacului suprafeţei solide şi aproximativ 40%..50% pentru cazul în care materialul se topeşte si este generat craterul de atac a condus la modelarea regimului pulsurilor laser. S-a căutat un regim format dintr-un tren de pulsuri cu intensităţi şi durate diferite. Câmpul termic produs de sursa laser a fost calculat utilizând metoda volumelor finite. Pe baza analizei distribuţiei temperaturii în baia de sudură s-au determinat volumele de control în care apar fenomene de vaporizare şi ionizare şi s-a obţinut atât forma geometrică a craterului produs de sursa de sudură cât şi distribuţia vitezelor pe suprafaţa acestuia. Datele astfel obţinute au fost utilizate în procesul de modelare cu volume finite, varianta celulelor marcate (MAC) a impulsurilor, distribuţiei reale a energiei în baia de sudură ca şi a formei geometrice a suprafeţei libere a acesteia (suprafaţa dintre baia de sudură şi perdeaua de gaze de protecţie).

Cuvinte cheie: sudare cu laser YAG, metoda volumelor finite, distribuţia temperaturii, baia de sudură.

ABSTRACT. In welding of thin Al sheet by a Nd:YAG laser beam, the mode of laser heating of the parts become extremely important. We can choose between continuum or pulse laser mode. In the case of continuum laser mode, the stability of welded shape geometry becomes difficult to be get. The little variations in laser spot power or position can generate instability of welded bead generated. In the laser pulse welding, the position of laser spot on the parts can be easy corrected in the pauses between two laser pulse trains. The importance of the laser pulse shapes become the most important parameter that get the welding penetration stability and welded bead shape. In order to evaluate the effect of laser pulse shape during Nd:YAG laser welding of thin Al sheet and to predict the welding performance by numerical simulation, a three-dimensional VFM heat flow analysis and a 3D fluid and heat flow is presented for different laser pulse shapes and related welding parameters. The simulation results show that the welding stability is greatly affected by the modulation of laser pulse shape for the same laser energy and welding parameters

Keywords: YAG laser welding, numerical simulation, VFM heat flow analysis.

1. INTRODUCTION

In order to weld an Al alloy, concentrated energy should melt the welding region before the conduction away of thermal energy through the Al alloy. Therefore, laser welding is a very efficient way to weld Al alloys. Laser welding with a Nd: YAG laser, which has a short wave length present advantages in contrast with other laser sources, like CO₂ laser, since the short wave length gives smaller spot size and results in higher laser

beam absorbance on an Al surface. In the case of low welding speed, the laser shooting condition is not so critical; the welded pools generate overlapping, but at a fast welding speed the situation the situation become different. During the pulse duration, the laser beam moves to the welding front but overall energy density for melting is low. Thus, high peak power is needed for fast welding, and then the related pulse duration and frequency should be changed. High peak power is disadvantageous for the controlling of melt pool

overheating, which induces vaporization. The advantages of modeling the laser pulse and his modulation shape can be used to prevent welding defects.

2. THEORETICAL BACKGROUND

2.1. Physical model

The illustration of the welding geometry is shown in figure 1. The pulsed Nd:YAG laser beam is focused on the surface of a butt joint; and the welding speed is constant. The laser beam absorbance increases with the specimen temperature, since the laser beam absorbance on a metal surface is a function of temperature. When the metal is melted, the metal phase no longer has a crystal structure but an amorphous phase. If the metal phase changes to the amorphous phase, the laser beam absorbance increases faster. Thus the laser beam absorbance on Al is adapted as approximate values at the given conditions. It is assumed that the laser beam absorbance is about 8% at room temperature and reaches 50% at the melting point. ⁽²⁾ The thermal conductivity and specific heat of Al are functions of temperature. In the calculation of temperature distribution by VFM simulation in this work and the temperature dependencies of conductivity and viscosity were considered in computer simulation. Also the latent heat of melting and freezing was considered in the computer simulation by the temperature recovery method. ⁽³⁾ In this simulation, laser beam energy density was not sufficiently high enough to form keyholes, which would cause deep penetration welding. Thus the laser beam does not penetrate deep into molten pool by the keyhole mechanism. In the computer simulation calculation, the size of the model was 10mm in length, 4.7 mm in width and 2mm in the thickness; the mesh number of elements was about 294,000. One element size was approximately 100 μm × 100 μm × 100 μm and the adaptive mesh method will be used in the area of focused laser beam spot size was about 300 μm × 300 μm. The above assumptions were summarized as given below and were considered in the computer simulation calculation:

- the laser beam absorbance, thermal conductivity and specific heat were dependent upon the temperature of the specimen, and the density of the specimen was constant;
- the effect of plasma was not considered but the radiation heat loss was considerate;
- the phase change was taken into account by the temperature recovery method;

- the melt temperature was sustained below the evaporation point and the evaporation heat loss was taken into account for the mass removal;
- the viscosity of the melting is temperature dependent;
- the free surface loses heat by radiation and the convection heat loosed is neglected;
- the convection heat exchange between the melt and solid phase is expressed based on Re and Pr numbers.

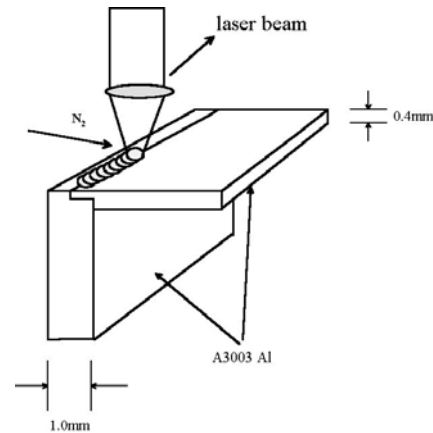


Fig. 1. Aspect of geometrical welded parts.

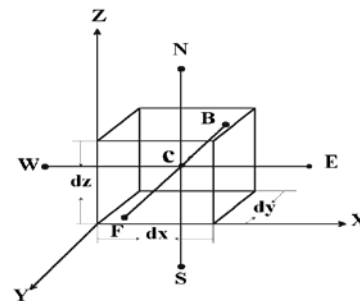


Fig. 2. Symbols for Finite Volume.

2.2. Governing equation and Boundary condition

General form of heat flow equation. The numerical simulation was conducted by the three-dimensional transient problem.

Although the specimen has a complex shape, the simplified geometry is adapted and the partial differential equation for heat transfer is given in the following equation (1),

$$\rho C \frac{\partial T}{\partial t} = \sum Q_i + \lambda \left(\frac{\partial^2 T}{\partial x^2} + \frac{\partial^2 T}{\partial y^2} + \frac{\partial^2 T}{\partial z^2} \right) + \rho_s \frac{\partial f_s}{\partial t} L_s \quad (1)$$

where T is temperature, x , y , and z are the coordination directions, respectively, λ is thermal conductivity, ρ is the density, C_p is the heat capacity, and t is time. The generalized equation from the control volume method, which was adapted for explicit method based on operator theory, is given in the following equation (2).

$$[e]_{mnl,isd}^{exp} = [\alpha_{xi} \quad 1 - n_x \alpha_x - n_y \alpha_y - n_z \alpha_z + \sum \beta_{SC} \quad \alpha_{x2} \quad \alpha_{y1} \quad \alpha_{y2} \quad \alpha_{z1} \quad \alpha_{z2}]$$

$$\varphi = \frac{\Delta t}{C \cdot \rho} Q_i$$

$$[L]_{ARC} = [\varphi_{Ax1} \quad \varphi \quad \varphi_{Ax2} \quad \varphi_{Ay1} \quad \varphi_{Ay2} \quad \varphi_{Az1} \quad \varphi_{Az2}]$$

$$[e]_{m,n,l,isd}^{exp} \cdot \begin{bmatrix} T_{m-1,n,l}^p \\ T_{m,n,l}^p \\ T_{m+1,n,l}^p \\ T_{m,n-1,l}^p \\ T_{m,n+1,l}^p \\ T_{m,n,l-1}^p \\ T_{m,n,l+1}^p \end{bmatrix} \pm [L]_{CV} \cdot \begin{bmatrix} T_{\infty,SC1} \\ 0 \\ T_{\infty,SC2} \\ T_{\infty,SC3} \\ T_{\infty,SC4} \\ T_{\infty,SC5} \\ T_{\infty,SC6} \end{bmatrix} \pm$$

$$[L]_{RD} \cdot \begin{bmatrix} T_{\infty,SC1} \\ 0 \\ T_{\infty,SC2} \\ T_{\infty,SC3} \\ T_{\infty,SC4} \\ T_{\infty,SC5} \\ T_{\infty,SC6} \end{bmatrix} + [L]_{ARC} \cdot \begin{bmatrix} T_{ASc1} \\ T_A \\ T_{ASc2} \\ T_{ASc3} \\ T_{ASc4} \\ T_{ASc5} \\ T_{ASc6} \end{bmatrix} = T_{m,n,l}^{p+\Delta t}$$

$$[L]_{CV} = [\beta_{CVx1} \quad 0 \quad \beta_{CVx2} \quad \beta_{CVy1} \quad \beta_{CVy2} \quad \beta_{CVz1} \quad \beta_{CVz2}]$$

$$\alpha_{xi} = \frac{\Delta t \lambda_x A_{CDxi}}{\Delta x C_p V} \quad \beta_{CVxi} = \frac{\Delta t h_{CV} A_{CVxi}}{\Delta x C_p V}$$

$$[L]_{RD} = [\beta_{RDx1} \quad 0 \quad \beta_{RDx2} \quad \beta_{RDy1} \quad \beta_{RDy2} \quad \beta_{RDz1} \quad \beta_{RDz2}]$$

$$\beta_{SCi} = \beta_{CVxi} + \beta_{RDxi} \quad \beta_{RDxi} = \frac{\Delta t h_{RD} A_{cvxi}}{\Delta x C_p V}$$

where: A_{CDxi} – conduction surface area control S_{Ci} , A_{CVxi} – convection surface area control S_{Ci} , V – finite volume; Δt – time stability interval analyse; Δx , Δy , Δz – mesh lengths; n_x – number of surfaces; C_p – specific heat; ρ – density; $\beta_{CVi,j,k}$ – thermal resistant coefficient of element of $A_{i,j,k}$ – $[L]_{CV}$ convection operator; $[L]_{RD}$ – radiation operator; $A_{CV i,j,k}$ – area of control surface $A_{i,j,k}$; Q_i – heat input by laser inside the control volume.

Figure 2 shows the nomenclature of the control volume approach and a mesh divided by the inner nodal point method, which is convenient for a complex shape problem. The initial condition was defined that the temperature of the specimen was 293 K at the initial state as equation (3).

$$T = T_0(x, y, z) \text{ at } t = 0 \quad (3)$$

The forced convective heat transfer was considered in boundary, and the average convective heat transfer coefficient h_m within the entire region of the top and bottom surface was required for solving equation (2). The average convective heat transfer coefficient was obtained by following equation

$$h_m = (\lambda \times N_{uss}) / L$$

where λ is the thermal conductivity of air, N_{uss} is the Nusselt number and L the length of the element (Δx , Δy , Δz). The expression of the Nusselt number is.

$$N_{uss} = 0,036 \cdot Pr^{0,43} (Re^{0,8} - 17,4) + 297 \cdot Pr^{\frac{1}{3}} \quad (4)$$

The fixed temperature boundary condition was applied to the surface except for the upper and bottom surface region. If the entire mass of element was evaporated by a high power density of laser beam, the boundary condition was changed from conduction to convection in the reference element until the next step calculation. The fixed temperature of the molten element was assumed to sustain and the laser beam irradiated on the next element below the element, which was evaporated.

$$f(T) = \begin{cases} 0, & \text{if } T \leq T_s \\ \frac{T - T_s}{T_1 - T_s}, & \text{if } T_s < T < T_1 \\ 1, & \text{if } T \geq T_1 \end{cases} \quad (5)$$

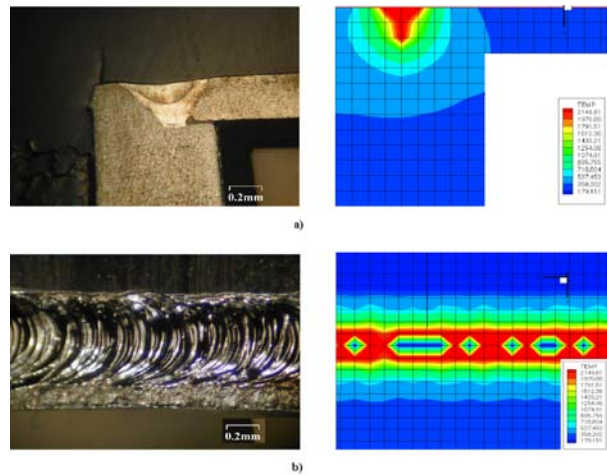


Fig. 3. Experimental results of welded region and simulation results of temperature distribution. Laser pulse shape with 3 levels. First: 6500 W, 0.2 msec; 2 nd: 4000W, 0.2 msec; 3 rd: 3000 W, 0.4 msec; frequency: 80Hz; scanning speed: 20 mm/sec; beam mode: multi-mode.
a – cross sectional view; b – top view.

Energy balance on the irradiated finite volume. The balance of energy on laser beam spot irradiated

finite volume take in account the energy lose in the phase change process, (melting, vaporization, ionization) the convection and pressure on the craters shape and finally the diffusion heat in the neighbors finite volumes.⁽¹⁶⁾

3. EXPERIMENTAL PROCEDURES

In order to compare the numerically simulated results with experimental results, the experiments were performed with a pulsed Nd:YAG laser, for which it was possible to modulate the laser pulse shape. The beam mode was multi-mode largely due to the optical fiber delivery system. The pulse shape modulations

used in this work with 3- divisions and the focused beam size was approx. 300 μm in diameter.

4. RESULTS AND DISCUSSION

The experiment was carried out with the same laser irradiation condition for the numerical simulation in order to verify the simulation. Figure 3 shows the experimental result and the simulated temperature distribution for multi-mode laser beam. The Figure 4 and Figure 5 show the results of temperature shape of pulse mode and longitudinal and transversal section of the experimental samples and the numerical results.

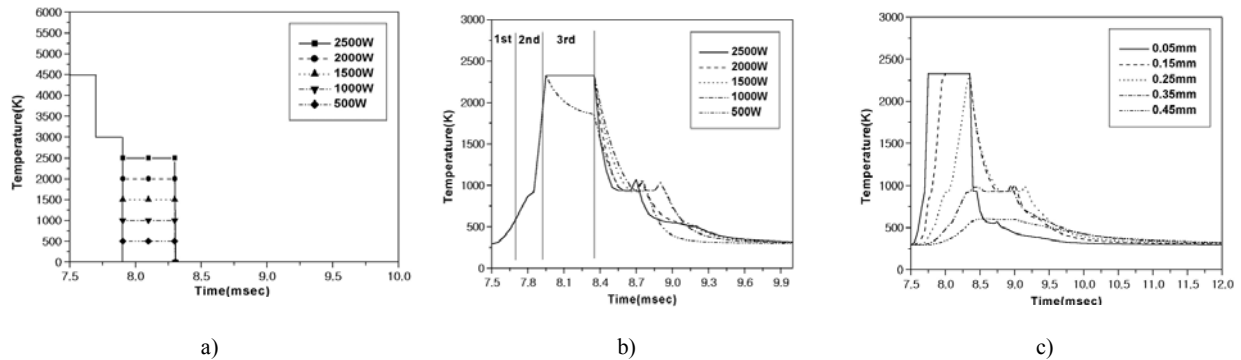


Fig. 4. Temperature induced by laser pulse shape.:

- a* – a laser pulse shape with 3 stage (1st: 4500 W, 0.2 msec; 2nd: 3000 W, 0.2 msec; 3rd: from 500 W to 2500 W, 0.4 msec);
- b* – temperature of the top surface as a function of time for various pulses shapes with different power in the third stage;
- c* – temperature variation as a function of time in the weld pool at different depths from the surface (2500 W in the 3rd stage).

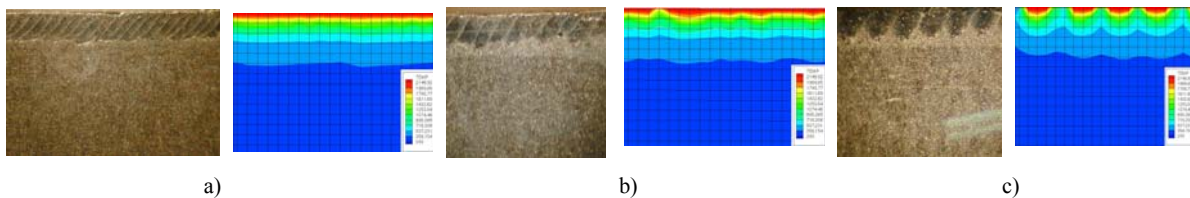


Fig. 5. Cross-sectional view of the weld region and simulated temperature profiles with

- various scanning speeds. (1st: 4500W, 0.2 msec, 2nd: 2800 W, 0.4 msec, 3rd: 1500 W, 0.2 msec, 110 Hz):
- a* – scanning speed: 10 mm/sec; *b* – scanning speed: 30 mm/sec; *c* – scanning speed: 50 mm/sec.

5. CONCLUSION

In welding of thin Al sheet by a pulsed Nd:YAG laser, the laser power level is the most influential in welding behavior. The simulation results show that the welding stability is greatly affected by the modulation of the laser pulse shape for same laser energy and welding parameters. As the rectangular laser pulse shape is modulated to have three stages with high, medium and low power level for first, second and third

stage respectively, more energy is absorbed in the melt pool and the cooling rate will be reduced. The simulated results give good agreement with experimental results, where sound weld shape and crack-free weld pool are obtained.

REFERENCES

[1] Yih-Fong Tzeng, *J. of Materials Processing*, Vol. 100, 2000; pp 163-170.

- [2] T. H. Kim, K. C. Chong, B. Y. Yoo, J. S. Lee: *J. of Material Science*, Vol. 30, No. 3, 1995; pp.784-792.
- [3] C.P. Hong and W. H. Baek, *J. of the Korean Inst. of Metals*, Vol.26, No.8, 1998; pp.810-821.
- [4] Y. Bayazitoglu and M. N. Ozisik, *Elements of Heat Transfer*, McGraw-Hill (New York), 1988; pp.209-214.
- [5] I. S. Leoveanu and Gh. Zgura, *Modelling the Heat and Fluid Flow in the Welded Pool from High Power Arc Sources*. Materials Science Forum Vols. 580-582 in June 2008. http://www.scientific.net/MSF/0-87849-383-2_443.pdf.
- [6] O. Grong. *Metallurgical Modelling of Welding*. Second Edition. The Institute of Materials. 1994.
- [7] H.S. Carslaw and J.C. Jaeger: *Conduction of Heat in Solids*; 1959, Oxford, Oxford University.
- [8] R. Hultgren, R.L. Orr, R.D. Anderson and K.K. Kelly: *Selected Values of Thermody. Prop.*; 1963, New York, J. Wiley & Sons.
- [9] A. A. Amsden and F. H. Harlow: *Report L.A. 4370*, Los Alamos Scientific Lab., (1970).
- [10] B. D. Nichols and C. W. Hirt: *J. Computational Physics*, 8 (1971), 434.
- [11] N.N. Rykalin, A.I. Pugin and V.A. Vasil'eva: *Weld. Prod.*, 1959, 6, 42-52.
- [12] O.R. Myhr and O. Grong: *Acta Metall. Mater.*, 1990, 38, 449-460.
- [13] N. Christensen: *Welding Metallurgy Compendium*, 1985, University of Trondheim,
- [14] CE. Jackson: *Weld. J.*, 1960, 39, 226s-230s.
- [15] O.M. Akselsen and G. Sagmo: *Technical Report STF34 A89147*, 1989, Trondheim (Norway),
- [16] I.S. Leoveanu, B-C Kim, Gh. Zgura, C.P. Hong: *The effect of laser beam mode considered by Numerical Simulation of Welding Performance for the Micro Welding of Thin Al Sheet by Nd: YAG. BRAMAT 2003 International Conference*. Brasov.